



# 1 Evident PM<sub>2.5</sub> Drops in the East of China due to the COVID-19 2 Quarantines in February

3 Zhicong Yin<sup>1,2,3</sup>, Yijia Zhang<sup>1</sup>, Huijun Wang<sup>1,2,3</sup>, Yuyan Li<sup>1</sup>

4 <sup>1</sup>Key Laboratory of Meteorological Disaster, Ministry of Education / Joint International Research Laboratory of Climate and  
5 Environment Change (ILCEC) / Collaborative Innovation Center on Forecast and Evaluation of Meteorological Disasters  
6 (CIC-FEMD), Nanjing University of Information Science & Technology, Nanjing, 210044, China

7 <sup>2</sup>Southern Marine Science and Engineering Guangdong Laboratory (Zhuhai), Zhuhai, 519080, China

8 <sup>3</sup>Nansen-Zhu International Research Centre, Institute of Atmospheric Physics, Chinese Academy of Sciences, Beijing, China

9 *Correspondence to:* Zhicong Yin (yinzhc@163.com)

10 **Abstract.** The top-level emergency response to the COVID-19 pandemic involved an exhaustive quarantine in China. The  
11 impacts of COVID-19 quarantine on the decline in fine particulate matter (PM<sub>2.5</sub>) were quantitatively assessed based on  
12 numerical simulations and observations in February. The stable meteorological conditions in February 2020 caused  
13 considerable PM<sub>2.5</sub> anomalies that were eliminated in advance. The contributions of routine emission reductions were also  
14 quantitatively extrapolated. The top-level emergency response substantially alleviated the level of haze pollution in the east of  
15 China. Although climate variability elevated the PM<sub>2.5</sub> by 29% (relative to 2020 observations), 59% decline related to COVID-  
16 19 pandemic and 20% decline from the expected pollution regulation dramatically exceeded the former in North China. The  
17 COVID-19 quarantine measures decreased the PM<sub>2.5</sub> in Yangtze River Delta by 72%. In Hubei Province where most pneumonia  
18 cases were confirmed, the impact of total emission reduction (72%) evidently exceeded the rising percentage of PM<sub>2.5</sub> driven  
19 by meteorology (13%).

20 **Keywords:** COVID-19, PM<sub>2.5</sub>, Emission Reduction, Climate Variability, Haze

## 21 1 Introduction

22 The COVID-19 pandemic devastatingly blew China in the beginning of 2020 (Luo, 2020; Xia et al., 2020; Cao et al.,  
23 2020). By April 2020, more than 84 thousand confirmed cases were reported by the National Health Commission of China,  
24 approximately 75% of which were confirmed in February (Fig. 1a). To effectively control the large spread of COVID-19  
25 pneumonia, stringent quarantine measures were implemented by the Chinese government and people themselves, including  
26 prohibiting social activities, shuttering industries, stopping transportation, etc. (Chen S. et al., 2020). The abovementioned  
27 emergency response measures were first carried out in Wuhan on 23 January, which resulted in the delayed arrival of COVID-  
28 19 in other cities by 2.91 days, and these response measures were in effect in all cities across China, thus limiting the spread  
29 of the COVID-19 epidemic in China (Tian et al., 2020). Since March 7, the number of newly confirmed cases in China has  
30 been nearly below 100. On the other hand, the COVID-19 quarantine measures greatly reduced anthropogenic emissions, and



31 therefore, the air quality in China was considerably improved (Wang P. et al., 2020). Chen K. et al. (2020) simply compared  
32 observations of atmospheric components before and during the quarantine and found that the concentration of fine particulate  
33 matter (PM<sub>2.5</sub>) in Wuhan decreased 1.4 µg/m<sup>3</sup>, but it decreased 18.9 µg/m<sup>3</sup> in 367 cities across China. Shi et al. (2020) quantified  
34 a 35% reduction of PM<sub>2.5</sub> on average during the COVID-19 outbreak compared to the pre-COVID-19 period. Huang et al.  
35 (2020) used comprehensive measurements and modeling to show that the haze during COVID-19 lockdown was driven by  
36 enhancements of secondary pollution, which offset reduction of primary emissions during this period in China. However, the  
37 impacts of meteorology on the air quality were neglected.

38 After the severe haze events of 2013, routine emission reductions resulted in an approximately 42% decrease in the annual  
39 mean PM<sub>2.5</sub> concentration between 2013 and 2018 in China (Cleaner air for China, 2019). In November 2019, the Ministry of  
40 Environmental Protection of China issued a series of Autumn-Winter Air Pollution Prevention and Management Plans  
41 indicating that the routine emission reductions would be conventionally implemented in the following winter (Ministry of  
42 Environmental Protection of China, 2019). Climate variability notably influences haze pollution in China (Yin and Wang 2016;  
43 Xiao et al., 2015; Zou et al., 2017), and the impacts are embodied by variations in surface wind, boundary layer height and  
44 moisture conditions (Shi et al., 2019; Niu et al., 2010; Ding et al., 2014). In winter 2017, the air quality in North China largely  
45 improved; however, the stagnant atmosphere in 2018 resulted in a major PM<sub>2.5</sub> rebound by weakening transport dispersion and  
46 enhancing the chemical production of secondary aerosols (Yin and Zhang 2020). Wang P. et al. (2020) applied the Community  
47 Multiscale Air Quality model to emphasize that the role of adverse meteorological conditions cannot be neglected even during  
48 the COVID-19 outbreak. Thus, high PM<sub>2.5</sub> concentrations were also observed in February 2020, which were mainly attributive  
49 to limited ventilation conditions and a high humidity (Ministry of Ecology and Environment of China, 2020).

50 As reported by the government, the mean ratio of work resumption in large industrial enterprises was approximately 90%  
51 in the east of China until the end of February (Fig. 1b). In this study, we attempted to quantify the impacts of the COVID-19  
52 pandemic on the observed PM<sub>2.5</sub> concentration in February 2020 when the quarantine measures were the strictest. The official  
53 7-day Chinese New Year holiday occurs in January and February and commonly accounts for approximately 25% of a month.  
54 From 2013–2020, there were only two years (2017 and 2020) when the official 7-day holiday occurred in January (Fig. 1c).  
55 Thus, to avoid the impacts of the Spring Festival, the observed PM<sub>2.5</sub> concentration in February 2017 (Fig. 1a) was adopted to  
56 calculate the PM<sub>2.5</sub> difference, which was decomposed into the results due to expected routine emission reductions, changing  
57 meteorology climate variability, and COVID-19 quarantines.

## 58 2 Datasets and methods

### 59 2.1 Data description

60 Monthly mean meteorological data from 2015 to 2020 were obtained from ERA5 reanalysis datasets, with a horizontal



61 resolution of  $0.25^{\circ} \times 0.25^{\circ}$ , including the geopotential height at 500 hPa (H500), zonal and meridional winds at 850 hPa, vertical  
62 wind from the surface to 150 hPa, and relative humidity at the surface (Dee et al., 2011).  $PM_{2.5}$  concentration data from 2015  
63 to 2020 were acquired from the China National Environmental Monitoring Centre (<http://beijingair.sinaapp.com/>).

## 64 **2.2 GEOS-Chem description and experimental design.**

65 We used the GEOS-Chem model (<http://acmg.seas.harvard.edu/geos/>) to simulate the  $PM_{2.5}$  concentration, driven by  
66 MERRA-2 assimilated meteorological data (Gelaro et al., 2017). The nested grid over China ( $15^{\circ}N$ – $55^{\circ}N$ ,  $75$ – $135^{\circ}E$ ) had a  
67 horizontal resolution of  $0.5^{\circ}$  latitude by  $0.625^{\circ}$  longitude and consisted of 47 vertical layers up to 0.01 hPa. The GEOS-Chem  
68 model included the fully coupled  $O_3$ – $NO_x$ –hydrocarbon and aerosol chemistry module with more than 80 species and 300  
69 reactions (Bey et al., 2001; Park et al., 2004). The  $PM_{2.5}$  components simulated in the GEOS-Chem model included sulfate,  
70 nitrate, ammonium, black carbon and primary organic carbon, mineral dust, and sea salt. At present, GEOS-Chem model has  
71 been widely used, and historical changes in air quality in China were also examined through modeling studies. Using the  
72 GEOS-Chem model, Yang et al. (2016) found an increasing trend of winter  $PM_{2.5}$  concentrations during 1985–2005, 80% of  
73 which due to anthropogenic emissions and 20% due to meteorological conditions. Dang et al. (2019) showed that this model  
74 could capture the spatial and temporal variations in severe winter haze in China and obtained increasing trends in the frequency  
75 and intensity of severe winter haze days in Beijing-Tianjin-Hebei from 1985-2017.

76 The  $PM_{2.5}$  concentration in February from 2015 to 2020 was simulated in this study. Due to delayed updates of the  
77 emission inventory, we used the emissions data of 2010  
78 (<http://geoschemdata.computecanada.ca/ExtData/HEMCO/AnnualScalar>) and 1985 (M. Li et al., 2017) for the simulations,  
79 which represented high- and low-emission scenarios, respectively. In total, we conducted two sets of numerical experiments  
80 to drive the GEOS-Chem simulations, one combining the meteorological conditions from 2015 to 2020 with fixed emissions  
81 in 1985 and the other with fixed emissions in 2010, which could determine the stability of simulated results. To further identify  
82 the reliability of the GEOS-Chem simulation, we focused on whether the simulations could capture the roles of meteorological  
83 changes in February 2020 under a substantial reduction in emissions because of COVID-19 quarantines. In North China (NC),  
84 Yangtze River Delta (YRD) and Hubei Province (HB), the correlation coefficients between daily  $PM_{2.5}$  observations and  
85 simulated data under 2010 (1985) emission scenario reached 0.83 (0.82), 0.67 (0.63), and 0.79 (0.73), respectively. For example,  
86 in NC, the simulation could well simulate severe haze events (e.g., from 8–14 and 18–22 February) and good air quality events  
87 (e.g., from 15–19 February), reflecting that it has ability to accurately capture the change of meteorological conditions (Fig.  
88 S1).

## 89 **2.3 The method to quantify the influence of the COVID-19 quarantine.**

90 As mentioned above, we aimed to examine the impact of the COVID-19 quarantines on  $PM_{2.5}$  over the February 2017



91 level. The  $PM_{2.5}$  difference in February 2020 ( $PM_{dOBS}$ ) was decomposed into three parts: the impacts of changing meteorology  
92 ( $PM_{dM}$ ), expected routine emissions reductions ( $PM_{dR}$ ) and COVID-19 quarantines ( $PM_{dC}$ ), and the decomposition equation  
93 was  $PM_{dOBS} = PM_{dM} + PM_{dR} + PM_{dC}$ . That is,  $PM_{dC} = PM_{dOBS} - PM_{dM} - PM_{dR}$ . It should be noted that  $PM_{dC}$  is the impact  
94 of the COVID-19 quarantines over the situation whereby the pandemic did not occur and routine emission reductions  
95 conventionally were in effect. The value of  $PM_{dE}$  (i.e.,  $PM_{dR} + PM_{dC}$ ) was the total impact of the emission reductions in  
96 February 2020 over the 2017 level.

97 Simulated  $PM_{2.5}$  data driven by changing meteorology with two fixed-emissions (1985 and 2010) were employed to  
98 determine the ratio of  $PM_{dM}$  of each year/ $PM_{dOBS}$  in 2017. Depending on the GEOS-Chem simulations, we found that the  
99  $PM_{2.5}$  percentage due to changing meteorology remained nearly constant regardless of the emission level (Fig. S2), which was  
100 consistent with the results of Yin and Zhang (2020). For example, the percentages due to different meteorology between 2020  
101 and 2017 were 22.1% (21.4%), -1.2% (-0.7%) and 9% (8.2%) in NC, YRD and HB under the low (high) emissions (Fig. S2).  
102 The percentage under 2010 emission scenario was selected as the final percentage because the emissions from each sector in  
103 2010 were more similar to recent years, and thus was more reasonable. Then, through multiplication by this percentage,  $PM_{dM}$ ,  
104 with respect to the 2017 observations, can be quantified in each simulation grid (STEP 1).

105 From 2015 to 2019,  $PM_{dC} = 0$ ; thus,  $PM_{dR} = PM_{dOBS} - PM_{dM}$ . Here, we repeated STEP 1 to determine  $PM_{dM}$  in each  
106 year from 2015 to 2019 relative to 2017 (i.e.,  $PM_{dM} = 0$  in 2017). After removing the effect of meteorological conditions in  
107  $PM_{2.5}$  differences,  $PM_{dR}$  in all years except 2020 can also be calculated. According to many previous studies, the change in  
108 emissions resulted in a linear change in air pollution (Cai et al., 2017; Wang et al., 2019), therefore, we used the method of  
109 extrapolation to speculate the impact of routine emission reduction on  $PM_{2.5}$ . We performed linear extrapolation based on  
110 known  $PM_{dR}$  values from 2015 to 2019 to obtain  $PM_{dR}$  in 2020 (STEP 2, Fig. S3). In Beijing and Shanghai, for example,  
111  $PM_{2.5}$  fell by 23.1% and 26.6% due to routine emission reduction in 2019, respectively, compared with 2015. Zhou et al. (2020)  
112 indicated that emission reductions caused 20–26% decreases in winter in Beijing which has been translated into 5 years. Zhang  
113 et al.<sup>22</sup> also showed that the emission controls in Beijing-Tianjin-Hebei region have led to significant reductions in  $PM_{2.5}$  from  
114 2013 to 2017 of approximately 20% after excluding the impacts of meteorology. Geng et al. (2019) found a 20% drop in the  
115 main component of  $PM_{2.5}$  in the Yangtze River Delta from 2013 to 2017. These results are consistent with our extrapolations.  
116 Therefore, it is reasonable to obtain  $PM_{dR}$  by extrapolation after removing the meteorological conditions.

117 Through STEP 1 and STEP 2,  $PM_{dC}$  and  $PM_{dR}$ , respectively, in 2020 can be determined.  $PM_{dOBS}$  can be directly  
118 calculated from the observed data. After removing the influences of climate anomalies and routine emission reductions, the  
119 impact of COVID-19 quarantines on  $PM_{2.5}$  ( $PM_{dC}$ ) was extracted as  $PM_{dOBS} - PM_{dM} - PM_{dR}$  (STEP 3).



### 120 3 Results

121 The mean  $PM_{2.5}$  concentration in February 2020 was nearly below  $80 \mu\text{g}/\text{m}^3$  at the vast majority of sites in the east of  
122 China, which was much lower than before (Fig. S4). North China (NC) was still the most polluted region ( $>40 \mu\text{g}/\text{m}^3$ ), but the  
123  $PM_{2.5}$  concentrations in the Pearl River Delta (PRD) and Yangtze River Delta (YRD) were  $< 20 \mu\text{g}/\text{m}^3$  and  $< 40 \mu\text{g}/\text{m}^3$ ,  
124 respectively. Relative to the observations in February 2017, negative  $PM_{2.5}$  anomalies were centered in North China (NC),  
125 with values of approximately  $-60$  to  $-40 \mu\text{g}/\text{m}^3$  in southern Hebei Province and northern Henan Province (Fig. 2). In Hubei  
126 Province (HB), where the COVID-19 pneumonia cases were the most severe in February, the  $PM_{2.5}$  concentration was  $20\text{--}40$   
127  $\mu\text{g}/\text{m}^3$  lower than that in 2017. The  $PM_{2.5}$  differences were also negative in YRD and PRD. Therefore, how much did air  
128 pollution decrease due to the COVID-19 quarantines in February in east of China?

129 Climate variability notably influences the interannual-decadal variations in haze pollution as verified by both  
130 observational analysis (Yin et al., 2015) and GEOS-Chem simulations (Dang and Liao, 2019). Furthermore, Zhang et al. (2020)  
131 reported that meteorology contributes 50% and 78% of the wintertime  $PM_{2.5}$  reduction between 2017 and 2013 in the Beijing-  
132 Tianjin-Hebei (BTH) region and YRD, respectively. Therefore, it is necessary to remove the influences of climate anomalies  
133 before quantifying the contributions of the COVID-19 quarantines on the air quality. Based on the GEOS-Chem simulations,  
134  $PM_{dM}$  (i.e., the  $PM_{2.5}$  difference due to changing meteorology) was calculated between February 2020 and 2017 (see Methods).  
135 To the south of  $30^\circ\text{N}$ , most  $PM_{dM}$  values were negative with small absolute values, at  $< 10 \mu\text{g}/\text{m}^3$ . To the north of  $30^\circ\text{N}$ , the  
136  $PM_{dM}$  values were mostly positive, ranging from  $30\text{--}60 \mu\text{g}/\text{m}^3$  in BTH (Fig. 3a). The highest observed  $PM_{2.5}$  concentrations  
137 were  $274$ ,  $223$ , and  $303 \mu\text{g}/\text{m}^3$  in Beijing, Tianjin and Shijiazhuang, respectively. Although human activities had sharply  
138 decreased, severe haze pollution (e.g., 8–13 and 19–25 February) was not avoided, which was attributed to the stagnant  
139 atmosphere (Wang P. et al., 2020), and these severe haze events were also reproduced by the GEOS-Chem simulation (see  
140 Section 2.2 and Fig. S1). As shown in Figure 4a-b, the meteorological conditions in February 2020 were more favorable for  
141 the occurrence of haze pollution in NC. In the mid-troposphere, an anomalous anticyclone was located over NC and the Sea  
142 of Japan (Fig. 4a). These anticyclonic anomalies clearly stimulated anomalous southerlies over eastern China, which not only  
143 transported sufficient water vapor to NC but also overwhelmed the climatic northerlies in winter (Fig. 4b). In addition, the  
144 anomalous upward motion associated with anomalous anticyclones prevented the downward transportation of westerly  
145 momentum and preserved the thermal inversion layer over NC (Fig. S5). Particularly, in the stagnant days (i.e., 8–13 and 19–  
146 25 February), the East Asia deep trough shifted eastwards and northwards than climate mean, which steered the cold air to  
147 North Pacific instead of North China (Figure 4c). The climatic northerlies in February, related to East Asia winter monsoon,  
148 also turned to be south winds in the east of China (Figure 4d). The weakening surface winds and strong thermal inversion  
149 corresponded to weaker dispersion conditions, and the higher humidity indicated a favorable environment for the hygroscopic  
150 growth of aerosol particles.



151 Since 2013, the Chinese government has legislated and implemented stringent air pollution prevention and management  
152 policies that have clearly contributed to air quality improvement (Wang Y. et al., 2019). As mentioned above, without the  
153 COVID-19 pandemic, these emission reduction policies would certainly remain in effect in February 2020. Thus, we  
154 extrapolated  $PM_{dR}$  (i.e., the  $PM_{2.5}$  difference due to expected routine emission reductions) between February 2020 and 2017  
155 to isolate the impacts of the COVID-19 quarantines (i.e.,  $PM_{dC}$ ).  $PM_{dR}$  was mostly negative in the east of China (Fig. 3b).  
156 Because the impacts of meteorology were proactively removed, these negative values illustrated that routine emission  
157 reductions substantially reduced the wintertime  $PM_{2.5}$  concentration. The contributions of the emission reduction policies were  
158 the greatest in the south of BTH and were also remarkable in Hubei Province (Fig. 3b). Although the  $PM_{dR}$  of Beijing in 2016  
159 did not strictly comply with the pattern of monotonous decrease, which might be caused by the fluctuation of policy and its  
160 implementation, the value of  $PM_{dR}$  in 2020 relative to 2017 was  $-8.4 \mu\text{g}/\text{m}^3$  and was comparable to the  $11.5 \mu\text{g}/\text{m}^3$  reductions  
161 due to policy during 2013–2017 (Zhang et al., 2020). In Shanghai,  $PM_{dR}$  was  $-12.0 \mu\text{g}/\text{m}^3$  (Fig. 5), whose magnitude was  
162 proportional with assessments by Zhang et al. (2020), and the trend was nearly linear. The rationality of the extrapolations of  
163  $PM_{dR}$  was also proved in Section 2.3. The trend of  $PM_{dR}$  in Wuhan was  $-9.6 \mu\text{g}/\text{m}^3$  per year from 2015–2019, which indicated  
164 high efficiency of the emission reduction policies and resulted in large  $PM_{dR}$  values in 2020 (i.e.,  $-21.8 \mu\text{g}/\text{m}^3$ ).

165 By removing the impacts of meteorology and routine emission reduction policies, the change in  $PM_{2.5}$  due to the COVID-  
166 19 quarantines was quantitatively extracted. As expected, this severe pandemic caused dramatic slumps in the  $PM_{2.5}$   
167 concentration across China (Fig. 3c). Large  $PM_{dC}$  values (approximately  $-60$  to  $-30 \mu\text{g}/\text{m}^3$ ) were located in the high-polluted  
168 NC regions where intensive heavy industries were stopped and the traditional massive social activities and transportations  
169 around Chinese New Year were cancelled as part of the COVID-19 quarantine measures. To the south of  $30^\circ\text{N}$ , the impacts of  
170 the COVID-19 quarantines on the air quality were relatively weaker ( $-30 \sim 0 \mu\text{g}/\text{m}^3$ ) than those in the north, which was possibly  
171 related to the background conditions of air quality improvement. To reduce the assessment uncertainties,  $PM_{dC}$  was also  
172 recalculated based on the GEOS-Chem simulations with fixed emission in 1985, which represented a low emission scenario.  
173 As described in the Methods section, the results in Figure S6 are consistent with those in Figure 3c, showing a high robustness.  
174 Furthermore, the mean  $PM_{2.5}$  concentration decreases due to the COVID-19 quarantines in NC, HB and YRD were analyzed,  
175 which accounted for 59%, 26% and 72% of the observed February  $PM_{2.5}$  concentration in 2020, revealing clear regional  
176 differences (Fig. 6).

177 It should be noted that the sum of  $PM_{dR}$  and  $PM_{dC}$  (i.e.,  $PM_{dE}$ ) is the total contribution of the emission reduction in  
178 February 2020 with respect to 2017 (Fig. 3d). In NC, YRD and HB, the COVID-19 quarantines and routine emission reductions  
179 drove  $PM_{2.5}$  in the same direction. The mean  $PM_{2.5}$  decrease in NC, due to the total emission reduction, was  $-43.3 \mu\text{g}/\text{m}^3$ ,  
180 accounting for 79% of the observed February  $PM_{2.5}$  concentration in 2020 (Fig. 6). Although the absolute values of both  $PM_{dR}$   
181 and  $PM_{dC}$  in YRD were smaller than those in NC, the change percentage (92%) was larger because of the lower base  $PM_{2.5}$   
182 concentration. In HB, where more than 80% of the confirmed COVID-19 cases in China occurred and the cities were in



183 emergency lockdown, the total anthropogenic emissions were clearly limited, which resulted in a 72% decline in  $PM_{2.5}$  in the  
184 atmosphere (Fig. 6). In particular, if the anthropogenic emissions did not decline, the  $PM_{2.5}$  concentration in NC, YRD and HB  
185 would increase to nearly twice the current observation (Fig. 6), indicating significant contributions of human activities to the  
186 air pollution in China.

187 The declines of  $PM_{2.5}$  seemed not to be directly proportional to the almost complete shutoff of vehicle traffics and  
188 industries, that is, the reduction ratio of  $PM_{2.5}$  concentrations were smaller than that of precursor emissions (Wang et al., 2020).  
189 The unexpected air pollutions during the marked emission reductions were closely related to the stagnant air flow, enhanced  
190 productions of secondary aerosols, and uninterrupted residential heating, power plants and petrochemical facilities (Le et al.,  
191 2020). The partial impacts of stagnant meteorological conditions have been explained earlier (Fig. 4). In Wuhan, the  $PM_{2.5}$   
192 remained the main pollutant during the city lockdown and the high level of sulphur dioxide ( $SO_2$ ) may be related to the  
193 increased domestic heating and cooking (Lian et al., 2020). In North China, large reductions of primary aerosols were observed,  
194 but the decreases in secondary aerosols were much smaller (Sun et al., 2020; Shi et al., 2020). Because of break-off  
195 transportations, reduced nitrogen oxide ( $NO_x$ ) increased the concentrations of ozone and nighttime nitrate ( $NO_3$ ) radical  
196 formations. The increased oxidizing capacity in the atmosphere enhanced the formation of secondary particulate matters  
197 (Huang et al., 2020). Thus, the non-linear relationship of emission reduction and secondary aerosols also partially contributed  
198 to the haze during the COVID-19 lockdown. Although the  $PM_{2.5}$  dropped much, marked air pollutions also occurred during  
199 this unique experiments that the human emissions were sharply closed. This implied reconsiderations of policy for pollution  
200 controls and necessity to cut off secondary productions of particulate matters (Le et al., 2020; Huang et al., 2020).

#### 201 **4 Conclusions and discussion**

202 In the beginning of 2020, the Chinese government implemented top-level emergency response measures to contain the  
203 spread of COVID-19. The traditional social activities surrounding Chinese New Year, industrial and transportation activities,  
204 etc. were prohibited, which effectively reduced the number of confirmed cases in China. Concomitantly, anthropogenic  
205 emissions, which are the fundamental reason for haze pollution, were dramatically reduced by the COVID-19 quarantine  
206 measures. In this study, we employed observations and GEOS-Chem simulations to quantify the impacts of the COVID-19  
207 quarantines on the air quality improvement in February 2020 after removing the contributions of expected routine emission  
208 reductions and climate variability. Although the specific influences varied by the region, the COVID-19 quarantines  
209 substantially decreased the haze pollution level in the east of China (Fig. 6). In North China, the meteorological conditions  
210 were stagnant that enhanced the  $PM_{2.5}$  concentration by 30% (relative to the observations in 2020). In contrast, the expected  
211 routine emissions reductions and emergency COVID-19 quarantine measures resulted in an 80% decline. In YRD, the impacts  
212 of meteorology were negligible but the COVID-19 quarantines decreased  $PM_{2.5}$  by 72%. In Hubei Province, the impact of the



213 total emission reduction (72%) evidently exceeded the  $PM_{2.5}$  increase due to meteorological conditions (13%). In March, due  
214 to the continued control of the COVID-19, the quarantines measures still contributed to the negative anomalies of the observed  
215  $PM_{2.5}$  between 2020 and 2017 (Figure 7a). Because the activities in production and life have been gradually resumed in March,  
216 the  $PM_{2.5}$  drops caused by the COVID-19 quarantines became weaker compared with February (Fig. 7b, c). The contributions  
217 of  $PM_{dC}$  to the change of  $PM_{2.5}$  concentration in NC, YRD and HB declined from 32.2, 21.0 and 12.1  $\mu\text{g}/\text{m}^3$  in February to  
218 7.0, 2.4 and 6.7  $\mu\text{g}/\text{m}^3$  in March respectively.

219 Because of the common update delay of the emission inventory, we employed a combined analysis consisting of statistical  
220 and numerical methods. We strictly demonstrated the rationality of this method, mainly based on the relatively constant  
221 contribution ratio of changing meteorology under the different emissions (Yin and Zhang 2020), and the  $PM_{2.5}$  drops due to  
222 COVID-19 quarantines which calculated based on the GEOS-Chem simulations with fixed emissions of 1985 were also  
223 relatively stable. Gaps between the results and reality still exist, which requires further numerical experiments when the  
224 emission inventory is updated. During the calculation process, the  $PM_{dM}$  is based on 2010 emissions, which are more  
225 representative of the emissions of each sector in recent years. The calculated  $PM_{2.5}$  percentages due to changing meteorology  
226 are relatively stable regardless of the emission level, but the result is obtained by numerical simulations, with certain  
227 uncertainty. When calculating the  $PM_{dR}$  in 2020, we use the method of extrapolation. Although the result is consistent with  
228 others observational and numerical studies (Geng et al., 2019; Zhang et al., 2020; Zhou et al., 2019), it is still conjectures rather  
229 than true values. In fact, the actual emission reduction effect is still considerable (Fig. 3d), in line with the increasingly  
230 strengthened emission reduction policies in recent years. Furthermore, we separated the effects of meteorology and emission  
231 reduction on  $PM_{2.5}$ , not taking into account the possible interaction between these two factors. These issues need to be  
232 examined in the future studies of the respective effects of emissions and meteorological conditions on  $PM_{2.5}$  over eastern China.  
233 Studies estimated that thousands of deaths were prevented during the quarantine because of the air pollution decrease (Chen  
234 K. et al., 2020). However, medical systems were still overstressed, and transportation to hospitals also decreased. Furthermore,  
235 the deaths related to air pollution were almost all due to respiratory diseases (Wang et al., 2001), and their corresponding  
236 medical resources were also further stressed by COVID-19. Therefore, the mortality impacted by the air pollution reduction  
237 during the COVID-19 outbreak should be comprehensively assessed in future work.

238

239

240

241

242

243

244





245

246

247 **Data availability.** Monthly mean meteorological data are obtained from ERA5 reanalysis data archive:  
248 <https://cds.climate.copernicus.eu/cdsapp#!/search?type=dataset>. PM<sub>2.5</sub> concentration data are acquired from the China  
249 National Environmental Monitoring Centre: <http://beijingair.sinaapp.com/>. The emissions data of 1985 can be downloaded  
250 from <http://geoschemdata.computecanada.ca/ExtData/HEMCO/AnnualScalar/>, and that of 2010 can be obtained from MIX:  
251 <http://geoschemdata.computecanada.ca/ExtData/HEMCO/MIX>.

252

#### 253 **Acknowledgements**

254 The National Natural Science Foundation of China (41991283, 9174431 and 41705058), the funding of Jiangsu innovation &  
255 entrepreneurship team, and the special project “the impacts of meteorology on large-scale spread of influenza virus” from CIC-  
256 FEMD supported this research.

257

#### 258 **Authors' contribution**

259 Wang H. J. and Yin Z. C. designed and performed researches. Zhang Y. J. simulated the PM<sub>2.5</sub> by GEOS-Chem model and Li  
260 Y. Y. did the statistical analysis. Yin Z. C. prepared the manuscript with contributions from all co-authors.

261

#### 262 **Competing interests**

263 The authors declare no conflict of interest.

264

265

266

267

268



269 **References**

- 270 Bey, I., Jacob, D. J., Yantosca, R. M., Logan, J. A., Field, B. D., Fiore, A. M., Li, Q. B., Liu, H. G. Y., Mickley, L. J., and  
271 Schultz, M. G.: Global modeling of tropospheric chemistry with assimilated meteorology: Model description and evaluation,  
272 *J. Geophys. Res. Atmos.*, 106, 23073–23095, <https://doi.org/10.1029/2001jd000807>, 2001.
- 273 Cai, S., Wang, Y., Zhao, B., Wang S., Chang, X., and Hao, J.: The impact of the “Air Pollution Prevention and Control Action  
274 Plan” on PM<sub>2.5</sub> concentrations in Jing-Jin-Ji region during 2012–2020, *Sci. Total Environ.*, 580, 197–209, 2017.
- 275 Cao, W., Fang, Z., Hou, G., Han, M., Xu X., and Dong, J.: The psychological impact of the COVID-19 epidemic on college  
276 students in China, *Psychiat. Res.*, 287, 112934, 2020.
- 277 Chen, S., Yang, J., Yang W., Wang, C., and Till, B.: COVID-19 control in China during mass population movements at New  
278 Year, *Lancet*, 395(10226), 764–766, 2020.
- 279 Chen, K., Wang, M., Huang, C., Patrick, L., and Paul, T.: Air Pollution Reduction and Mortality Benefit during the COVID-  
280 19 Outbreak in China, *MedRxiv*, <https://doi.org/10.1101/2020.03.23.20039842>, 2020.
- 281 Cleaner air for China, *Nat. Geosci.*, 12, 497–497, <https://doi.org/10.1038/s41561-019-0406-7>, 2019.
- 282 Dang, R., and Liao, H.: Severe winter haze days in the Beijing-Tianjin-Hebei region from 1985 to 2017 and the roles of  
283 anthropogenic emissions and meteorology, *Atmos. Chem. Phys.*, 19, 10801–10816, 2019.
- 284 Dee, D. P., Uppala, S. M., Simmons, A. J., Berrisford, P., Poli, P., Kobayashi, S., Andrae, U., Balmaseda, M. A., Balsamo, G.,  
285 Bauer, P., Bechtold, P., and Beljaars, A. C. M.: The ERA Interim reanalysis: configuration and performance of the data  
286 assimilation system, *Q. J. Roy. Meteor. Soc.*, 137, 553–597, <https://doi.org/10.1002/qj.828>, 2011.
- 287 Ding, Y., and Liu, Y.: Analysis of long-term variations of fog and haze in China in recent 50 years and their relations with  
288 atmospheric humidity, *Sci. China Ser. D.*, 57, 36–46, 2014.
- 289 Xiao, D., Li, Y., Fan, S., Zhang, R., Sun, J., and Wang, Y.: Plausible influence of Atlantic Ocean SST anomalies on winter haze  
290 in China. Plausible influence of Atlantic Ocean SST anomalies on winter haze in China, *Theor. Appl. Climatol.*, 122, 249–257,  
291 2015.
- 292 Gelaro, R., McCarty, W., Suarez, M. J., Todling, R., Molod, A., Takacs, L., Randles, C. A., Darmenov, A., Bosilovich, M. G.,  
293 Reichle, R., Wargan, K., Coy, L., Cullather, R., Draper, C., Akella, S., Buchard, V., Conaty, A., da Silva, A. M., Gu, W., Kim,  
294 G. K., Koster, R., Lucchesi, R., Merkova, D., Nielsen, J. E., Partyka, G., Pawson, S., Putman, W., Rienecker, M., Schubert, S. D.,  
295 Sienkiewicz, M., and Zhao, B.: The Modern-Era Retrospective Analysis for Research and Applications, Version 2 (MERRA2),  
296 *J. Climate*, 30, 5419–5454, <https://doi.org/10.1175/jcli-d-160758.1>, 2017.
- 297 Geng, G., Xiao, Q., Zheng, Y., Tong, D., Zhang, Y., Zhang, X., Zhang, Q., He, H., and Liu, Y.: Impact of China’s Air Pollution  
298 Prevention and Control Action Plan on PM<sub>2.5</sub> chemical composition over eastern China, *Sci. China Ser. D.*, 62, 1872–1884,  
299 <https://doi.org/10.1007/s11430-018-9353-x>, 2019.



300 Huang, X., Ding, A., Gao, J., Zheng, B., Zhou, D., Qi, X., Tang, R., Ren, C., Nie, W., Chi, X., Wang, J., Xu, Z., Chen, L., Li,  
301 Y., Che, F., Pang, N., Wang, H., Tong, D., Qin, W., Cheng, W., Liu, W., Fu, Q., Chai, F., Davis, S., Zhang, Q., and He, K.:  
302 Enhanced secondary pollution offset reduction of primary emissions during COVID-19 lockdown in China, *Natl. Sci. Rev.*,  
303 *nwaa* 137, 2020.

304 Kalnay, E., Kanamitsu, M., Kistler, R., Collins, W., Deaven, D., Gandin, L., Iredell, M., Saha, S., White, G., Woollen, J., Zhu,  
305 Y., Leetmaa, A., Reynolds, R., Chelliah, M., Ebisuzaki, W., Higgins, W., Janowiak, J., Mo, K. C., Ropelewski, C., Wang, J.,  
306 Jenne, R., and Joseph, D.: The NCEP/NCAR 40-year reanalysis project, *B. Am. Meteorol. Soc.*, 77, 437–471,  
307 [https://doi.org/10.1175/1520-0477\(1996\)077<0437:TNYRP>2.0.CO;2](https://doi.org/10.1175/1520-0477(1996)077<0437:TNYRP>2.0.CO;2), 1996.

308 Le, T., Wang, Y., Liu, L., Yang, J., Yung, Y. L., Li, G., and John, H.: Unexpected air pollution with marked emission reductions  
309 during the covid-19 outbreak in China, *Science*, 369(6504), eabb7431, 2020.

310 Li, M., Zhang, Q., Kurokawa, J.-I., Woo, J.-H., He, K., Lu, Z., Ohara, T., Song, Y., Streets, D. G., Carmichael, G. R., Cheng,  
311 Y., Hong, C., Huo, H., Jiang, X., Kang, S., Liu, F., Su, H., and Zheng, B.: MIX: a mosaic Asian anthropogenic emission  
312 inventory under the international collaboration framework of the MICS-Asia and HTAP, *Atmos. Chem. Phys.*, 17, 935–963,  
313 <https://doi.org/10.5194/acp-17-935-2017>, 2017.

314 Lian, X., Huang, J., Huang, R., Liu, C., and Zhang, T.: Impact of city lockdown on the air quality of COVID-19-hit of Wuhan  
315 city, *Sci. Total Environ.*, 742, 140556, 2020.

316 Luo, Z.: The impact of new outbreak on economy, capital market and national governance and its response, *Finance Economy*,  
317 2020(2), 8–15, 2020.

318 Ministry of Environmental Protection of China.  
319 [http://www.mee.gov.cn/xxgk/xxgk05/201903/t20190306\\_694550.html](http://www.mee.gov.cn/xxgk/xxgk05/201903/t20190306_694550.html), 2019.

320 Ministry of Environmental Protection of China.  
321 [http://www.mee.gov.cn/xxgk/xxgk15/202002/t20200211\\_762584.html](http://www.mee.gov.cn/xxgk/xxgk15/202002/t20200211_762584.html), 2020.

322 Niu, F., Li, Z., Li, C., Lee, K., and Wang, M.: Increase of wintertime fog in China: Potential impacts of weakening of the  
323 Eastern Asian monsoon circulation and increasing aerosol loading, *J. Geophys. Res.*, 115, D7, 2020.

324 Park, R.: Natural and transboundary pollution influences on sulfate-nitrate-ammonium aerosols in the United States:  
325 Implications for policy, *J. Geophys. Res. Atmos.*, 109, D15204, 2004.

326 Shi, X., and Brasseur, G.: The Response in Air Quality to the Reduction of Chinese Economic Activities during the COVID  
327 Outbreak, *Geophys. Res. Lett.*, 2020, 47, 2020.

328 Shi, Y., Hu, F., Lü R., and He, Y.: Characteristics of urban boundary layer in heavy haze process based on beijing 325m tower  
329 data, *Atmos. Oceanic Sci. Lett.*, 12, 41–49, 2019.

330 Sun, Y., Lei, L., Zhou, W., Chen, C., and Worsnop, D. R.: A chemical cocktail during the COVID-19 outbreak in Beijing,  
331 China: Insights from six-year aerosol particle composition measurements during the Chinese New Year holiday. *Sci. Total*



- 332 Environ., 140739, 2020.
- 333 Tian, H., Liu, Y., Li, Y., Wu, C., Chen, B., Kraemer, M., Li, B., Cai, J., Xu, B., Yang, Q., Wang, B., Yang, P., Cui, Y., Song, Y.,  
334 Zheng, P., Wang, Q., Bjornstad, O., Yang, R., Grenfell, B., Pybus, O., Dye, C.: An investigation of transmission control  
335 measures during the first 50 days of the COVID-19 epidemic in China, *Science*, eabb6105, 2020.
- 336 Wang, H., and Jin, Y.: The Study on Air Pollution Effects on the Mechanism of Respiratory System. *Science of Travel*  
337 *Medicine*, 007(002), 29–33, 2001.
- 338 Wang, P., Chen, K., Zhu, S., Wang, P., and Zhang, H.: Severe air pollution events not avoided by reduced anthropogenic  
339 activities during COVID-19 outbreak, *Resour. Conserv. Recy.*, 158, <http://doi:10.1016/j.resconrec.2020.104814>, 2020.
- 340 Wang, Y., Li, W., Gao, W., Liu, Z., Tian, S., Shen, R., Ji, D., Wang, S., Wang, L., Tang, G., Tao, S., Cheng, M., Wang, G., Gong,  
341 Z., Hao, J., and Zhang, Y.: Trends in particulate matter and its chemical compositions in China from 2013–2017, *Sci. China*  
342 *Ser. D.*, 62(12), 1857–1871, 2019.
- 343 Xia, J., and Feng, X.: Impacts of COVID-19 epidemic on tourism industry and related countermeasures, *Chinese Business and*  
344 *Market*, 34(3), 3–10, 2020.
- 345 Yang, Y., Liao, H., and Lou, S.: Increase in winter haze over eastern China in recent decades: Roles of variations in  
346 meteorological parameters and anthropogenic emissions, *J. Geophys. Res. Atmos.*, 121, 13050–  
347 13065, <https://doi.org/10.1002/2016jd025136>, 2016.
- 348 Yin, Z., and Wang, H.: The relationship between the subtropical Western Pacific SST and haze over North-Central North China  
349 Plain, *Int. J. Climatol.*, 36, 3479–3491, 2016.
- 350 Yin, Z., Wang, H., and Guo, W.: Climatic change features of fog and haze in winter over North China and Huang-Huai Area,  
351 *Sci. China Ser. D.*, 58, 1370–1376, 2015.
- 352 Yin, Z., and Zhang, Y.: Climate anomalies contributed to the rebound of PM<sub>2.5</sub> in winter 2018 under intensified regional air  
353 pollution preventions, *Sci. Total Environ.*, 726, 138514, 2020.
- 354 Zhang, X., Xu, X., Ding, Y., Liu, Y., Zhang, H., Wang, Y., Zhong, J.: The impact of meteorological changes from 2013 to 2017  
355 on PM<sub>2.5</sub> mass reduction in key regions in China, *Sci. China Ser. D.*, 62, 1885–1902, [https://doi.org/10.1007/s11430-019-9343-](https://doi.org/10.1007/s11430-019-9343-3)  
356 [3](https://doi.org/10.1007/s11430-019-9343-3), 2020.
- 357 Zhou, W., Gao, M., He, Y., Wang, Q., Xie, C., Xu, W., Zhao, J., Du, W., Qiu, Y., Lei, L., Fu, P., Wang, Z., Worsnop, D., Zhang,  
358 Q., and Sun, Y.: Response of aerosol chemistry to clean air action in Beijing, China: Insights from two-year ACSM  
359 measurements and model simulations, *Environ. Pollut.*, 255, 113345, 2019.
- 360 Zou, Y., Wang, Y., Zhang, Y., and Koo, J.: Arctic sea ice, Eurasia snow, and extreme winter haze in China, *Sci. Adv.*, 3,  
361 e1602751, 2017.
- 362
- 363



364 **Figure Captions**

365 Figure 1. (a) Variation in existing confirmed cases (bar) and the ratio of accumulated confirmed cases to total confirmed cases  
366 (black line) in China. (b) The ratio of work resumption in large industrial enterprises in the east of China. (c) Time of the  
367 official 7-days holiday of Chinese New Year from 2013 to 2020.

368 Figure 2. Differences in the observed  $PM_{2.5}$  (unit:  $\mu\text{g}/\text{m}^3$ ) in February between 2020 and 2017. The black boxes indicate the  
369 locations of North China (NC), the Yangtze River Delta (YRD) and Hubei Province (HB).

370 Figure 3.  $PM_{2.5}$  difference (unit:  $\mu\text{g}/\text{m}^3$ ) in February between 2020 and 2017 (a) due to changing meteorology ( $PM_{dM}$ ), (b) due  
371 to expected routine emission reductions ( $PM_{dR}$ ), (c) due to the COVID-19 quarantines ( $PM_{dC}$ ), and (d) due to the total emission  
372 reduction ( $PM_{dE} = PM_{dR} + PM_{dC}$ ).

373 Figure 4. Differences in the observed atmospheric circulation in February between 2020 and 2017, including (a) geopotential  
374 potential height at 500 hPa (unit: gpm), (b) wind at 850 hPa (arrows; unit: m/s), surface relative humidity (shading; unit: %).  
375 The atmospheric circulations in the stagnant days (e.g., from 8–13 and 19–25 February 2020) were also showed, including (c)  
376 geopotential potential height at 500 hPa (shading) and its climate mean in February (contour), and (d) wind at 850 hPa (black  
377 arrows), its climate mean (blue arrows) and the increased surface relative humidity (shading, stagnant days minus climate  
378 mean).

379 Figure 5. Variation in  $PM_{dR}$  (unit:  $\mu\text{g}/\text{m}^3$ ) with respect to the February 2017 level in Beijing, Shanghai and Wuhan from 2015  
380 to 2019.  $PM_{dR}$  in 2020 was linearly extrapolated from that in the 2015–2019 period. The dotted line is the linear trend.

381 Figure 6. Contributions of  $PM_{dM}$  (orange bars with hatching),  $PM_{dR}$  (purple bars with hatching) and  $PM_{dC}$  (blue bars with  
382 hatching) to the change in  $PM_{2.5}$  concentration (unit:  $\mu\text{g}/\text{m}^3$ ) between 2020 and 2017 in the three regions. The observed  $PM_{2.5}$   
383 concentration in February 2017 (black) and 2020 (gray) was also plotted, and the expected  $PM_{2.5}$  concentration without the  
384 COVID-19 quarantine is indicated by black hollow bars. The contribution ratios of the three factors (relative to the  $PM_{2.5}$   
385 observations in 2020) are also indicated on the corresponding bars.

386 Figure 7. (a) Differences in the observed  $PM_{2.5}$  (unit:  $\mu\text{g}/\text{m}^3$ ) in March between 2020 and 2017. (b) Contributions of  $PM_{dC}$  to  
387 the change in  $PM_{2.5}$  concentration (unit:  $\mu\text{g}/\text{m}^3$ ) between 2020 and 2017 and (c) the contribution ratios of  $PM_{dC}$  (relative to the  
388  $PM_{2.5}$  observations in 2020) in March (blue) and February (red) in the three regions.

389

390

391

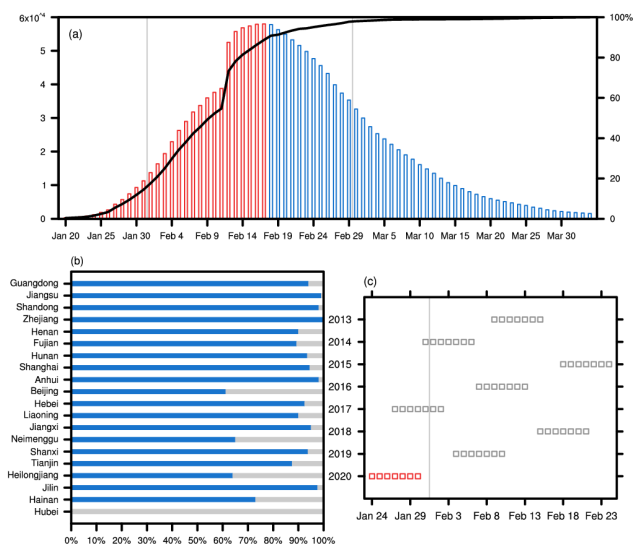
392

393

394

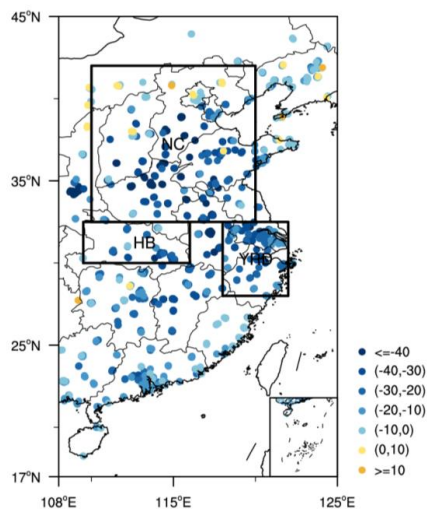


395 **Figures**



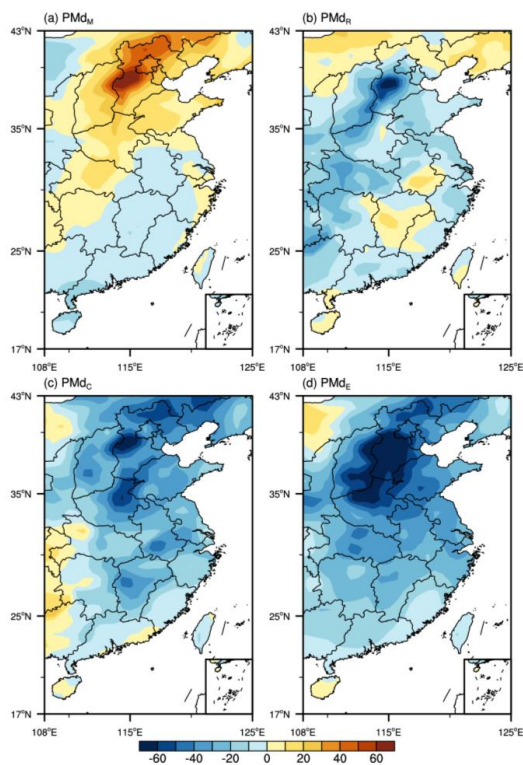
396

397 **Figure 1.** (a) Variation in existing confirmed cases (bar) and the ratio of accumulated confirmed cases to total confirmed cases  
398 (black line) in China. (b) The ratio of work resumption in large industrial enterprises in the east of China. (c) Time of the  
399 official 7-days holiday of Chinese New Year from 2013 to 2020.



400

401 **Figure 2.** Differences in the observed  $PM_{2.5}$  (unit:  $\mu g/m^3$ ) in February between 2020 and 2017. The black boxes indicate the  
402 locations of North China (NC), the Yangtze River Delta (YRD) and Hubei Province (HB).

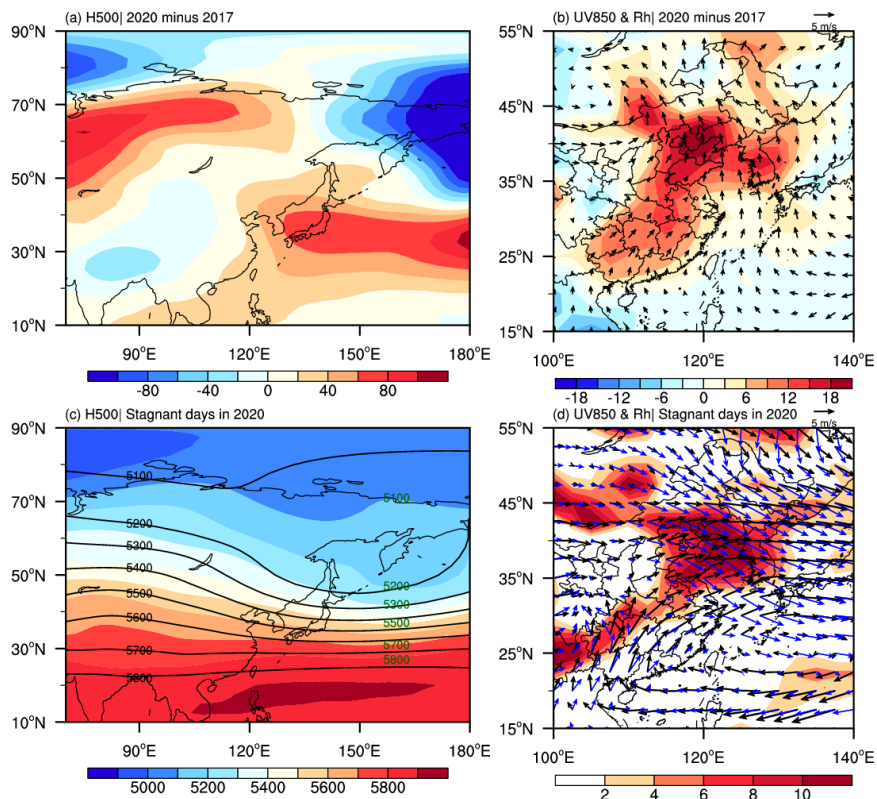


403

404 **Figure 3.**  $\text{PM}_{2.5}$  difference (unit:  $\mu\text{g}/\text{m}^3$ ) in February between 2020 and 2017 (a) due to changing meteorology ( $\text{PMd}_M$ ), (b)  
405 due to expected routine emission reductions ( $\text{PMd}_R$ ), (c) due to the COVID-19 quarantines ( $\text{PMd}_C$ ), and (d) due to the total  
406 emission reduction ( $\text{PMd}_E = \text{PMd}_R + \text{PMd}_C$ ).

407

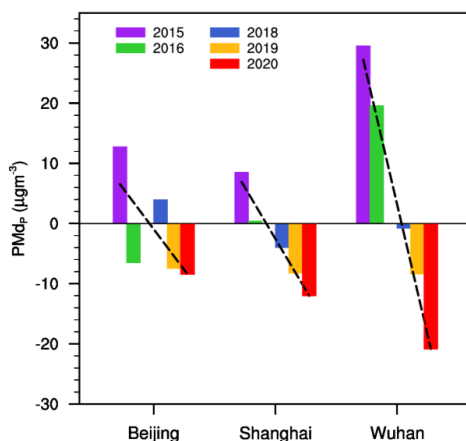
408



409

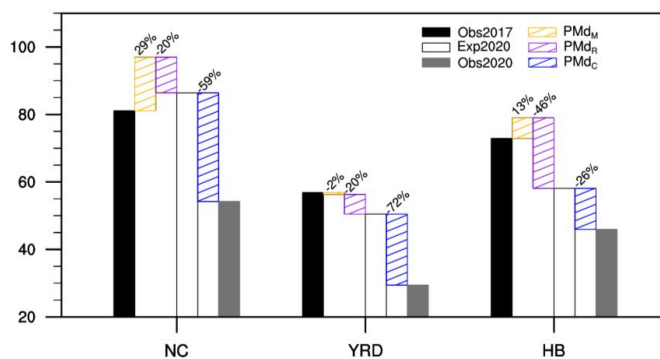
410 **Figure 4.** Differences in the observed atmospheric circulation in February between 2020 and 2017, including (a) geopotential  
411 potential height at 500 hPa (unit: gpm), (b) wind at 850 hPa (arrows; unit: m/s), surface relative humidity (shading; unit: %).  
412 The atmospheric circulations in the stagnant days (e.g., from 8–13 and 19–25 February 2020) were also showed, including (c)  
413 geopotential potential height at 500 hPa (shading) and its climate mean in February (contour), and (d) wind at 850 hPa (black  
414 arrows), its climate mean (blue arrows) and the increased surface relative humidity (shading, stagnant days minus climate  
415 mean).





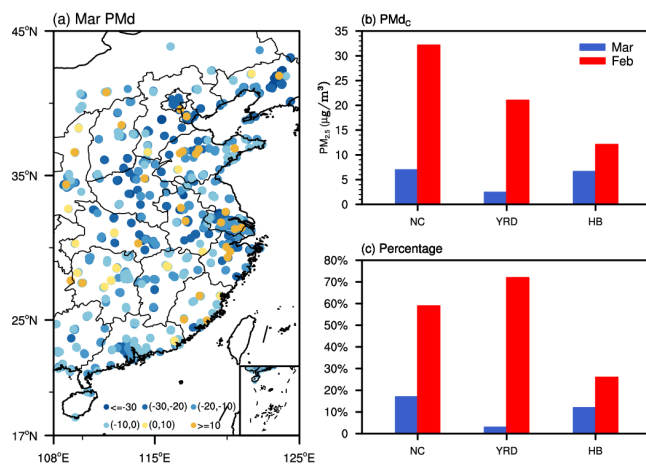
416

417 **Figure 5.** Variation in  $PMd_R$  (unit:  $\mu g/m^3$ ) with respect to the February 2017 level in Beijing, Shanghai and Wuhan from 2015  
 418 to 2019.  $PMd_R$  in 2020 was linearly extrapolated from that in the 2015–2019 period. The dotted line is the linear trend.



419

420 **Figure 6.** Contributions of  $PMd_M$  (orange bars with hatching),  $PMd_R$  (purple bars with hatching) and  $PMd_C$  (blue bars with  
 421 hatching) to the change in  $PM_{2.5}$  concentration (unit:  $\mu g/m^3$ ) between 2020 and 2017 in the three regions. The observed  $PM_{2.5}$   
 422 concentration in February 2017 (black) and 2020 (gray) was also plotted, and the expected  $PM_{2.5}$  concentration without the  
 423 COVID-19 quarantine is indicated by black hollow bars. The contribution ratios of the three factors (relative to the  $PM_{2.5}$   
 424 observations in 2020) are also indicated on the corresponding bars.



425

426 **Figure 7.** (a) Differences in the observed PM<sub>2.5</sub> (unit:  $\mu\text{g}/\text{m}^3$ ) in March between 2020 and 2017. (b) Contributions of PMd<sub>C</sub> to  
427 the change in PM<sub>2.5</sub> concentration (unit:  $\mu\text{g}/\text{m}^3$ ) between 2020 and 2017 and (c) the contribution ratios of PMd<sub>C</sub> (relative to the  
428 PM<sub>2.5</sub> observations in 2020) in March (blue) and February (red) in the three regions.

429

430